

## **CREEP BEHAVIOR OF ROTATING FGM DISC WITH LINEAR AND HYPERBOLIC THICKNESS PROFILES**

**Dharmpal Deepak<sup>1</sup>, Manish Garg<sup>2</sup> and V.K. Gupta<sup>1</sup>**

<sup>1</sup>*Department of Mechanical Engineering, Punjabi University, Patiala-147002, India.  
E-mail: guptavk\_70@yahoo.co.in*

<sup>2</sup>*Department of Physics, S.D. College, Barnala, Punjab, 148101, India.*

*(Received September 26, 2014)*

**ABSTRACT.** Mathematical model has been developed to investigate steady state creep in a variable thickness rotating disc made of functionally graded Al-SiCp. The SiCp content in the disc is assumed to decrease from the inner to outer radius. The creep behavior of the disc material is described by threshold stress based law with a stress exponent of 5. The stresses and strain rates in the disc are estimated by solving creep constitutive equations along with the equilibrium equation for a rotating disc. The stresses and strain rates have been estimated for similar FGM discs with three different thickness profiles *i.e.* constant thickness, linearly varying thickness and hyperbolic varying thickness. The FGM disc having hyperbolic thickness profile exhibits the lowest stresses and strain rates compared linear or constant thickness disc. The tangential and radial strain rates in FGM discs with linear and hyperbolic thickness profiles are respectively lower by about two and three orders of magnitude when compared to a constant thickness FGM disc. The FGM discs having linear and hyperbolic thickness profiles possess lesser chances of distortion due to relatively uniform distribution of radial strain rate.

**Key words:** Modeling, Creep, Rotating Disc, Functionally Graded Material, Thickness Profile.

### **INTRODUCTION**

Rotating discs are the most critical part of rotors, turbines, flywheel etc. [1-3]. In most of these applications, the disc has to operate under elevated temperature and is simultaneously subjected to high stresses caused by disc rotation at high speed [4]. As a result of severe mechanical and thermal loadings, the disc undergoes creep deformations, which may severely affect its performance [2, 5-8]. Metal matrix composites containing aluminium/ aluminium alloy matrix reinforced with ceramics like SiC offer excellent mechanical properties such as high specific strength and stiffness and high temperature stability. Therefore these composites are suitable for rotating disc applications involving thermo-mechanical loadings [2, 9]. In general, the distribution of reinforcement in composites is kept uniform. Functionally Graded Materials (FGMs) are special types of composites in which the content of constituent phases is continuously varied as a function of position coordinates along certain dimension(s), so as

to achieve desired variations in required properties [10, 11]. As a result, the FGMs can be tailored to sustain under severe thermo-mechanical loading conditions, as observed in a rotating disc [12].

The problem of creep in rotating FGM disc operating under thermo-mechanical loadings has attracted the interest of many researchers. SINGH and RAY [13] studied the steady state creep behavior of a constant thickness rotating disc made of isotropic functionally graded Al-SiCp and operating under a constant elevated temperature. The distribution of SiCp was assumed to decrease linearly from the inner to outer radius of the disc. The steady state creep response of the FGM disc is observed to be significantly superior to a similar disc having uniform distribution of SiCp. GUPTA *et al.* [14] analyzed steady state creep in a constant thickness rotating FGM (Al-SiCp) disc operating under a radial thermal gradient. The analysis indicates that for the assumed linear distribution of SiCp, the steady-state strain rates in the FGM disc are significantly lower than those observed in an isotropic disc having uniform distribution of SiCp. YOU *et al.* [15], assuming Young's modulus, density and thermal expansion coefficient to be functions of the radial coordinate, obtained closed form solutions for rotating FGM disc operating at uniform temperature. CHEN *et al.* [16] presented three-dimensional analytical solutions for a rotating disc made of transversely isotropic FGM. BAYAT *et al.* [17] performed thermo-elastic analysis of a rotating FGM disc of constant thickness with small and large deflections. It is observed that for certain values of grading index ( $n$ ) of the material properties, mechanical responses in an FGM disc can be smaller than a homogenous disc. BAYAT *et al.* [18] further extended their analysis to obtain elastic solutions for rotating FGM discs having variable thickness. KORDKHEILI and NAGHDABADI [19] presented semi-analytical thermo-elastic solutions for solid and hollow rotating axi-symmetric FGM discs under plane stress condition.

ORCAN and ERASLAN [20] observed that the reduction in disc thickness increases its plastic limit angular velocity and reduces the magnitudes of stresses and deformations in the disc. JAHED *et al.* [21] pointed out that the use of variable thickness disc helps in minimizing the disc weight, as desired in aerospace applications. GUPTA *et al.* [22] also observed that a rotating disc having radially decreasing density and thickness from the inner to outer radius is much safer in comparison to a flat disc having variable density. ALI *et al.* [23] obtained elastic solutions for a variable thickness rotating FGM disc. The material properties were represented by combination of two sigmoid FGM. The effects of material grading index and disc geometry were investigated on the stresses and displacements. HASSANI *et al.* [24] analyzed stresses and strains in a variable thickness rotating disc with non-uniform material properties, subjected to thermo-elasto-plastic loading. THAKUR *et al.* [25] analyzed steady thermal stresses in a rotating disc, mounted on a shaft, having density variation parameter by using Seth's transition theory. It is noticed that the disc made of compressible material requires higher percentage increase in angular speed to become fully-plastic as compared to disc made of incompressible material.

The literature consulted so far reveals that the studies concerning creep in rotating FGM disc having variable thickness are rather scant. Therefore, it is decided to investigate the steady state creep in a rotating disc made of functionally graded Al-SiCp and having varying thickness profiles. The creep stresses and creep rates have been estimated in FGM discs having linearly and hyperbolically varying thickness profiles. The results obtained are compared with those estimated for a constant thickness FGM disc to see the impact of varying disc profile on its creep performance.

## DISTRIBUTION OF REINFORCEMENT

The distribution of SiCp in the FGM disc is assumed to decrease linearly from the inner to outer radius. Therefore, the density and creep parameters, being dependent on the content of reinforcement, of the FGM disc will also vary radially. The content of SiCp,  $V(r)$ , at any radius  $r$  in the FGM disc is given by,

$$V(r) = V_{\max} - \frac{(r-a)}{(b-a)}(V_{\max} - V_{\min}) = \delta_1 - \delta_2 r \quad (1)$$

where,  $\delta_1 = (V_{\max} + a\delta_2)$ ,  $\delta_2 = \frac{(V_{\max} - V_{\min})}{(b-a)}$  and  $V_{\max}$  and  $V_{\min}$  are respectively the maximum and minimum SiCp content at the inner and outer radii of the disc respectively.

It is assumed that the total content of SiCp is equal in all the FGM discs chosen in this study. Therefore, the average SiCp content in the disc ( $V_{av}$ ) can be estimated as,

$$V_{av} = \frac{\int_a^b 2\pi r h(r) V(r) dr}{\pi(b^2 - a^2)t} \quad (2)$$

The inner ( $a$ ) and outer ( $b$ ) radii of the disc are assumed respectively as 31.75 mm and 152.4 mm and the average thickness ( $t$ ) of the disc is taken as 25.4 mm, as assumed in our previous work [2, 14].

## DISC THICKNESS PROFILES

In this study, the analysis has been conducted for variable thickness FGM disc having linear and hyperbolic thickness profiles.

For FGM disc having linearly varying thickness, the thickness  $h(r)$  at any radius  $r$  is given by,

$$h(r) = h_b + 2c(b-r) \quad (3)$$

where  $c = \frac{(h_a - h_b)}{2(b-a)}$  and  $h_a$  and  $h_b$  are thickness of the FGM disc at  $r=a$  and  $r=b$  respectively.

Substituting  $h(r)$  and  $V(r)$  respectively from eqs. (1) and (3) into eq. (2), one may obtain the minimum SiCp content in linearly varying thickness disc as,

$$V_{\min} = \frac{V_{\max}(h_b b^2 - 2h_b a^2 + b^3 c - 5a^2 bc + ab^2 c + abh_b + 3a^3 c) - 3V_{av} t (b^2 - a^2)}{(abh_b + ab^2 c + a^2 h_b + a^2 bc - a^3 c - 2b^2 h_b - b^3 c)} \quad (4)$$

For the purpose of numerical computations, it is assumed that  $V_{\max} = 35\%$  and  $V_{av} = 20\%$ , therefore, one gets  $V_{\min} = 6.54\%$ .

In case of hyperbolic varying thickness disc, the thickness  $h(r)$  of the disk is assumed to vary radially according to the following equation,

$$h(r) = C_a r^k \quad (5)$$

Where  $k$  ( $= -0.5$ ) and  $C_a$  are the constants.

By equating the volume of hyperbolic disc with that of constant thickness disc, one obtains the value of  $C_a$  as,

$$C_a = \frac{1.5(b^2 - a^2)t}{2(b^{3/2} - a^{3/2})}$$

Substituting  $h(r)$  and  $V(r)$  respectively from eqs. (1) and (5) into eq. (2), one obtains the minimum SiCP content in the hyperbolic FGM disc as,

$$V_{\min} = V_{\max} - (b-a) [RV_{\max} - SV_{av}] \quad (6)$$

Where  $R = \frac{P}{Q}$ ,  $S = \frac{M}{Q}$ ,  $P = 2C_a (b^{3/2} - a^{3/2})$ ,  $Q = C_a \left[ \frac{2}{3}(b-a)b^{3/2} - \frac{4}{15}(b^{3/2} - a^{3/2}) \right]$  and  $M = \frac{(b^2 - a^2)t}{2}$

For  $V_{\max} = 35\%$  and  $V_{av} = 20\%$ , as assumed for linear thickness disc, one gets  $V_{\min} = 8.11\%$  for hyperbolically varying FGM disc.

## CREEP LAW AND CREEP PARAMETERS

In aluminium or its alloys based composites, undergoing steady state creep, the effective creep rate ( $\dot{\epsilon}$ ) is related to the effective stress ( $\bar{\sigma}$ ) through a well documented threshold stress ( $\sigma_0$ ) based creep law given by [26-27],

$$\dot{\epsilon} = A \left( \frac{\bar{\sigma} - \sigma_0(r)}{E} \right)^n \exp\left(\frac{-Q}{RT}\right) \quad (7)$$

where the symbols  $A$ ,  $n$ ,  $Q$ ,  $E$ ,  $R$  and  $T$  respectively denote structure dependent parameter, true stress exponent, true activation energy, temperature-dependent Young's modulus, gas constant and operating temperature.

The creep law, eq. (7), may alternatively be written as,

$$\dot{\epsilon} = [M(r)(\bar{\sigma} - \sigma_0)]^n \quad (8)$$

Where  $M(r) = \frac{1}{E} \left( A \exp\frac{-Q}{RT} \right)^{1/n}$  and  $\sigma_0$  are creep parameters depending on the type of material and the temperature ( $T$ ) of application.

In a composite, the dispersoid-size ( $P$ ) and content ( $V$ ) are the primary variables affecting these parameters. In this study, the values of  $M$  and  $\sigma_0$  have been extracted from the uniaxial creep results available for Al-SiCP [28], as reported in Table-1. The regression analysis has been performed for data given in Table 1, using DATAFIT software, to estimate the values of  $M$  and  $\sigma_0$ , at any radius ( $r$ ) of the FGM disc, in terms of SiCP size ( $P$ ), content of SiCP,  $V(r)$ , and operating temperature ( $T$ ). The developed regression equations, as reported elsewhere [12], are as below,

$$M(r) = 0.0288 - \frac{0.0088}{P} - \frac{14.0267}{T} + \frac{0.0322}{V(r)} \quad (9)$$

$$\sigma_0(r) = -0.084P - 0.023T + 1.185V(r) + 22.207 \quad (10)$$

In the present study, the stress exponent ( $n$ ) is selected as 5, the size ( $P$ ) of SiCP is taken as  $1.7 \mu\text{m}$  and the operating temperature ( $T$ ) is assumed to be  $623 \text{ K}$  over the entire disc, similar to that chosen in earlier work [12]. To obtain the distributions of stresses and strain rates in the FGM discs, the creep parameters are estimated from the regression eqs. (9) and (10).

## ANALYSIS

The generalized constitutive equations for creep in an isotropic composite disc under plane stress condition (*i.e.* axial stress,  $\sigma_z=0$ ) takes the following form when the reference frame is along the principal directions  $r, \theta$  and  $z$  of the disc [14],

$$\begin{aligned}\dot{\epsilon}_r &= \frac{\dot{\bar{\epsilon}}}{2\bar{\sigma}} [2\sigma_r - \sigma_\theta] \\ \dot{\epsilon}_\theta &= \frac{\dot{\bar{\epsilon}}}{2\bar{\sigma}} [2\sigma_\theta - \sigma_r] \\ \dot{\epsilon}_z &= \frac{\dot{\bar{\epsilon}}}{2\bar{\sigma}} [-\sigma_r - \sigma_\theta]\end{aligned}\quad (11)$$

where  $\dot{\epsilon}_r, \dot{\epsilon}_\theta$  and  $\dot{\epsilon}_z$  are the strain rates in  $r, \theta$  and  $z$  directions respectively and  $\sigma_r$  and  $\sigma_\theta$  are respectively the stresses in  $r$  and  $\theta$  directions.

The effective stress ( $\bar{\sigma}$ ) in a rotating disc under plane stress condition is given by [2],

$$\bar{\sigma} = \frac{1}{\sqrt{2}} [\sigma_\theta^2 + \sigma_r^2 + (\sigma_r - \sigma_\theta)^2]^{1/2} \quad (12)$$

Substituting  $\dot{\bar{\epsilon}}$  and  $\bar{\sigma}$  respectively from eqs. (8) and (12) into first equation amongst the set of eqs. (11), the radial strain rate ( $\dot{\epsilon}_r$ ) in the disc is obtained as,

$$\dot{\epsilon}_r = \frac{d\dot{u}_r}{dr} = \frac{[2x(r)-1]}{2[\{x(r)\}^2 - x(r)+1]^{1/2}} [M(r)\{\bar{\sigma} - \sigma_0(r)\}]^n \quad (13)$$

Where  $x = \sigma_r/\sigma_\theta$ ,  $\dot{u}_r = (du/dt)$  is the radial deformation rate and  $u$  is radial deformation in the disc.

Similarly, from the second equation amongst the set of eqs. (11), one obtains the tangential strain rate ( $\dot{\epsilon}_\theta$ ) in the disc,

$$\dot{\epsilon}_\theta = \frac{\dot{u}_r}{r} = \frac{[2-x(r)]}{2[\{x(r)\}^2 - x(r)+1]^{1/2}} [M(r)\{\bar{\sigma} - \sigma_0(r)\}]^n \quad (14)$$

From eqs. (13) and (14), one gets the tangential stress ( $\sigma_\theta$ ) in the disc as,

$$\sigma_\theta = \frac{\dot{u}_a^{1/n} \psi_1(r)}{M(r)} + \psi_2(r) \quad (15)$$

Where,

$$\psi_1(r) = \frac{\psi(r)^{1/n}}{[\{x(r)\}^2 - x(r)+1]^{1/2}}; \quad \psi_2(r) = \frac{\sigma_0(r)}{[\{x(r)\}^2 - x(r)+1]^{1/2}} \quad (16)$$

and,

$$\psi(r) = \frac{2[\{x(r)\}^2 - x(r)+1]^{1/2}}{r[2-x(r)]} \exp\left(\int_a^r \frac{\phi(r)}{r} dr\right) \quad (17)$$

Considering the equilibrium of forces acting on the FGM disc having varying thickness [29], one obtains,

$$\frac{d}{dr} [h(r)r\sigma_r] - h(r)\sigma_\theta + \rho(r)\omega^2 r^2 h(r) = 0 \quad (18)$$

Where  $\rho(r)$  is the density of composite disc at a radius  $r$ .

If the disc is assumed to be under free-free conditions i.e. the disc is connected to the shaft by means of splines, the following boundary conditions may be applied [14],

$$\sigma_r = 0 \text{ at } r = a \text{ and } \sigma_r = 0 \text{ at } r = b \quad (19)$$

Simplifying eq. (15) one gets,

$$\sigma_\theta = \frac{\frac{\psi_1(r)}{M(r)} \left[ A_0 \sigma_{av} - \int_a^b h(r) \psi_2(r) dr \right]}{\int_a^b \frac{h(r) \psi_1(r)}{M(r)} dr} + \psi_2(r) \quad (20)$$

Integrating the equilibrium eq. (18) between limits  $a$  to  $r$ , the radial stress  $\sigma_r$  in the FGM disc is estimated as,

$$\sigma_r = \frac{1}{h(r)r} \left[ \int_a^r h(r) \sigma_\theta dr - \omega^2 \left[ A_\rho I - B_\rho \left( \frac{(h_b + 2cb)(r^4 - a^4)}{4} - \frac{2c(r^5 - a^5)}{5} \right) \right] \right] \quad (21)$$

Where  $I (= \int_a^r hr^2 dr)$  is the polar moment of area of the disc element with the inner and outer radii respectively as  $a$  and  $r$ .

Once the distributions of  $\sigma_\theta$  and  $\sigma_r$  in the FGM disc are known, the strain rates ( $\dot{\epsilon}_r, \dot{\epsilon}_\theta$ ) in the disc are estimated from eqs. (13) and (14) respectively.

## RESULTS AND DISCUSSION

A computer code, based on the mathematical formulation presented in section 4, has been developed to estimate the distributions of stresses and strain rates in the FGM discs having linear and hyperbolic thickness profiles. For comparison, the results are also estimated for a similar FGM disc having uniform thickness.

Figure 1 shows the variation of thickness for three different FGM discs chosen in this study *viz* constant thickness FGM disc (disc 1), linearly varying thickness FGM disc (disc 2) and hyperbolically varying thickness FGM disc (disc 3). Figure 2 shows the distribution of reinforcement (SiCp) in various FGM discs. The SiCp content decreases from the inner to outer radius in hyperbolic and linear FGM discs (*i.e.* disc2 and disc3) while in uniform thickness FGM disc1 the content of SiCp remains 20 vol% over the entire radius. The maximum difference in SiCp content between disc2 and disc3 is 1.57 vol% at the outer radius. Figures 3(a) and 3(b) show respectively the variation of creep parameters  $M$  and  $\sigma_0$  in FGM discs. The value of parameter  $M$  in hyperbolic and linear FGM disc (*i.e.* disc2 and disc3) increases non-linearly with increasing radial distance. The increase observed in parameter  $M$  is attributed to decrease in particle content,  $V(r)$ , in disc2 and disc3, as one move from the inner to outer radius (Figure 2), as evident from eq. (9). On the other hand, the threshold stress,  $\sigma_0$ , shown in Figure 3(b), decreases with increasing radial distance, as observed for FGM disc2 and disc3. The threshold stress is higher in regions having more amount of SiCp compared to those having relatively lower SiCp content, as revealed from Figure 2 and eq. (10). Both the creep parameters,  $M$  and  $\sigma_0$ , observed in uniform thickness FGM disc1 remains constant due to uniform amount (20 vol%) of SiCp over the entire disc radius.

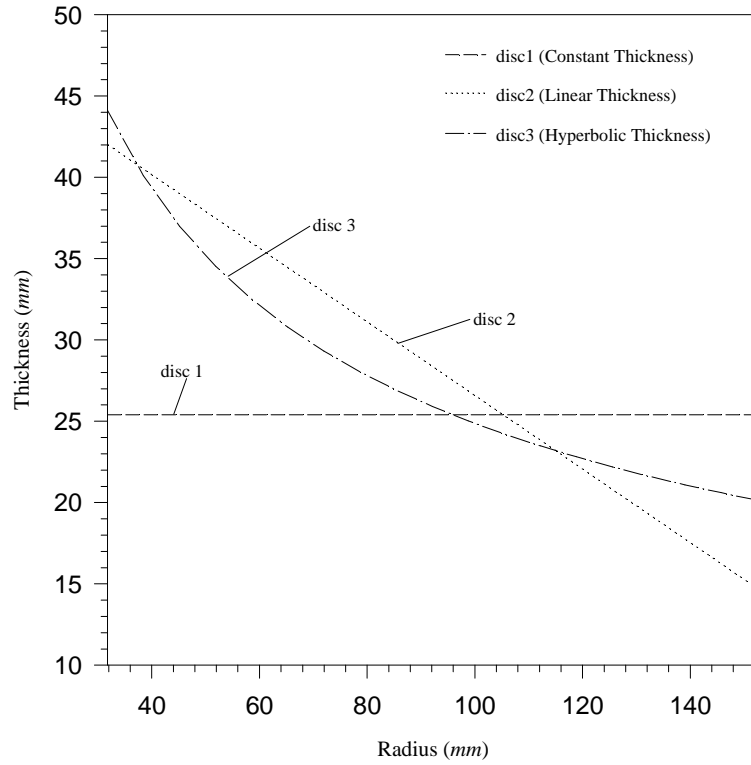


Figure 1. Disc thickness profiles of the FGM discs.

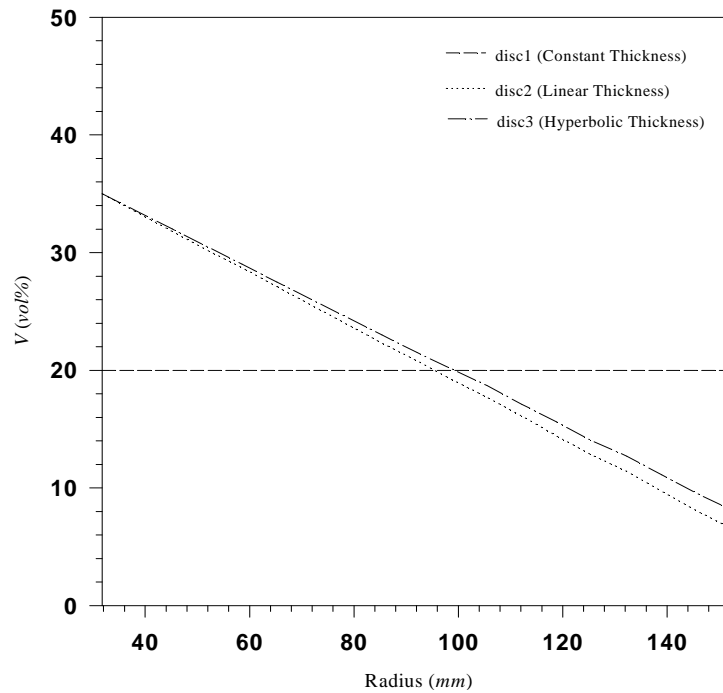


Figure 2. Variation of particle content in FGM discs.

Figures 4-8 show the effect of varying disc profile on the steady state creep behavior of the FGM discs. The radial stress, as shown in Figure 4, increases from zero at the inner radius, reaches a maximum, before becoming zero again at the outer radius, under the imposed boundary conditions given in eq. (19). The FGM disc2 having hyperbolic thickness profile exhibits the lowest radial stress over the entire radius as compared to any other FGM

discs. The radial stress in FGM disc3 is higher than the FGM disc2 but lower than the FGM disc1. The maximum difference observed in radial stress between uniform thickness disc1 and hyperbolic disc2 is about  $11.60 \text{ MPa}$  at a radius of  $78.67 \text{ mm}$ . The effect of varying disc thickness profile on tangential stress, Figure 5, is similar to that observed for radial stress in Figure 4. The tangential stress in hyperbolic disc2 is the lowest and the highest in constant thickness disc1. The effect of varying disc thickness profile is relatively higher towards the inner radius than observed at the outer radius. The maximum variation observed in tangential stress between constant thickness disc1 and hyperbolic disc3 is  $32.51 \text{ MPa}$  at the inner radius. The effect of thickness profile on effective stress in FGM disc, Figure 6, is similar to that observed for tangential stress in Figure 5. The hyperbolic disc2 again exhibits the lowest effective stress over the entire radius. The lower tangential and effective stresses observed towards the outer radius of hyperbolic disc2 is attributed to reduced centrifugal loading as a result of lower thickness of the hyperbolic disc2 than the constant thickness (disc1) and linear thickness (disc3) discs. At the inner radius, although the centrifugal force caused by disc rotation will increase due to increase in disc thickness, the simultaneous increase in disc cross-section area leads to reduce stresses near the inner radius of hyperbolic disc2 as compared to constant thickness disc1 and linear thickness disc3.

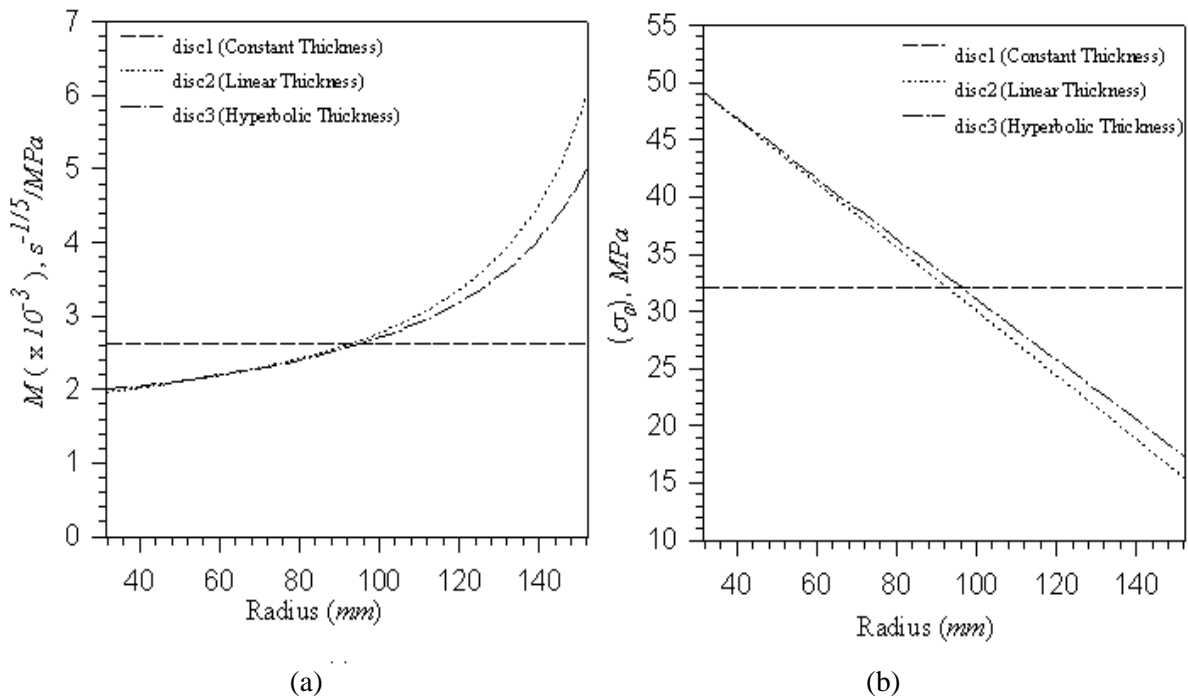


Figure 3. Variation of creep parameters in FGM discs.



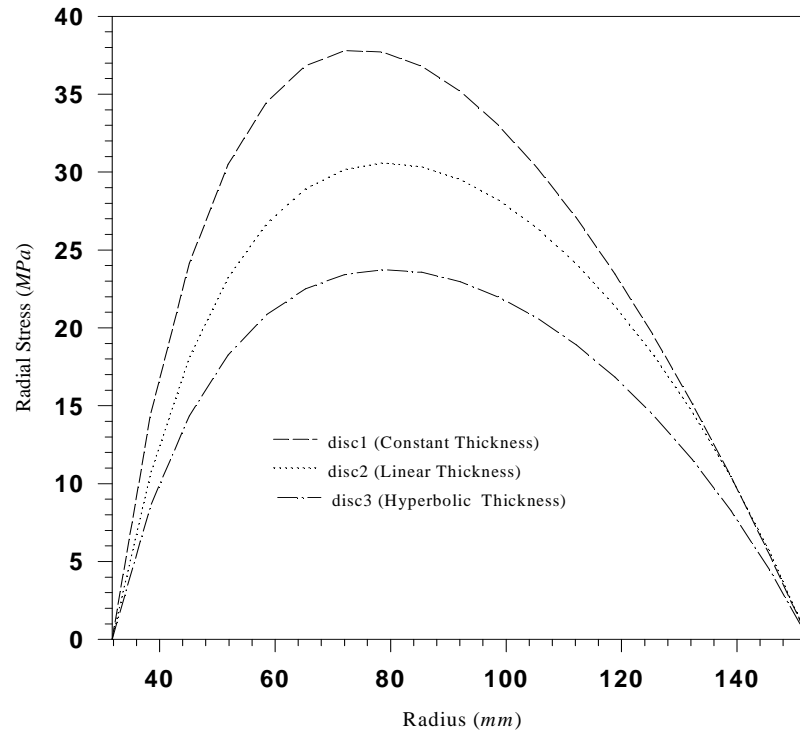


Figure 4. Effect of thickness profile on radial stress.

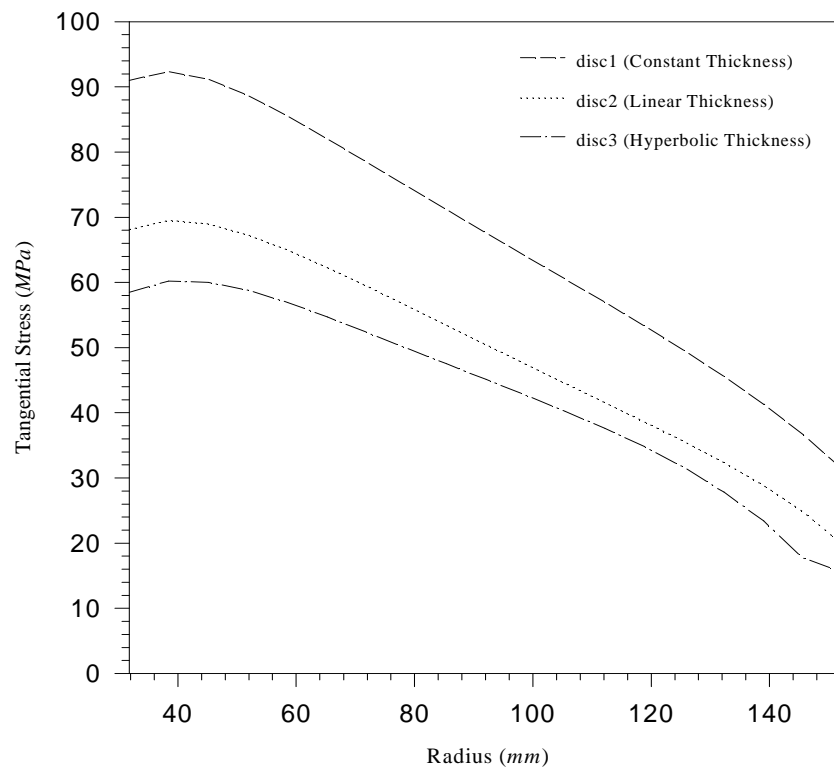


Figure 5. Effect of thickness profile on tangential stress.

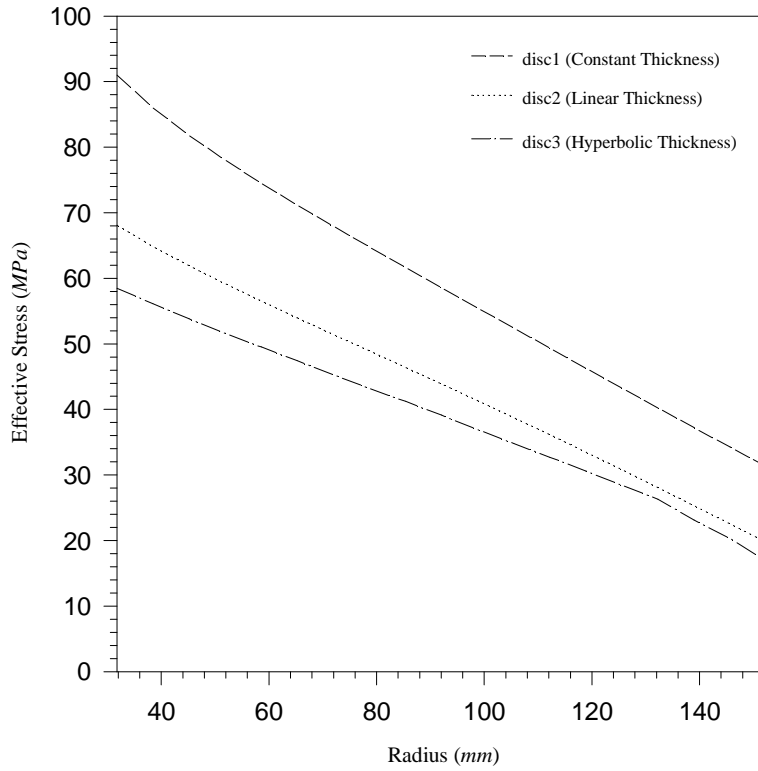


Figure 6. Effect of thickness profile on effective stress.

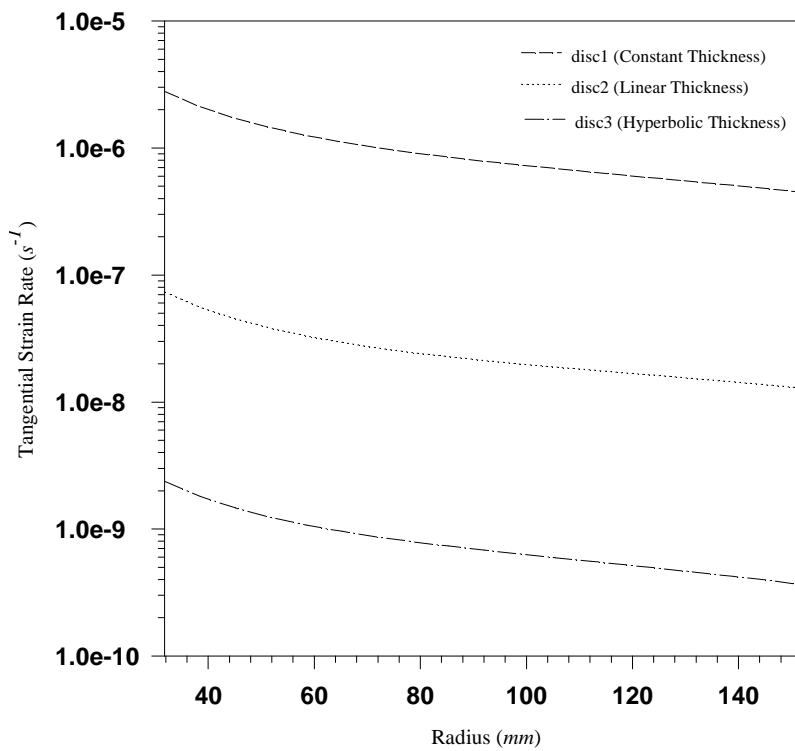


Figure 7. Effect of thickness profile on tangential strain rate.

The tangential strain rate, Figure 7, is the highest at the inner radius and goes on decreasing with increasing radial distance. The tangential strain rate is significantly affected by varying the disc profile. The tangential strain rate is the highest in uniform thickness disc1 and the lowest in hyperbolic disc2. The tangential strain rate in hyperbolic disc2 and linear disc3 is lower by about three and two orders of magnitude respectively than the constant thickness disc1. The effect of varying disc profile on radial strain rate, Figure 8, is similar to those observed for tangential strain rate in Figure 7. The radial strain rate in hyperbolic and linear FGM discs (*i.e.* disc2 and disc3) becomes relatively uniform than the constant thickness disc1, thereby reducing the chances of distortion in the FGM disc having variable thickness. In addition, the nature of radial strain rate in all the FGM discs becomes tensile in some region in the middle of the disc. Though, the magnitude of tensile radial strain rate is the lowest in FGM disc2. Towards the inner radius, the lower strain rates in hyperbolic disc2 than the constant thickness disc1 and linear disc3 is attributed to lower effective stress (Figure 6), lower value of  $M$  and higher value of  $\sigma_0$  (Figures 3a-3b), as is evident from eqs. (13)-(14). In spite of lower value of parameter  $M$  and higher value of  $\sigma_0$  towards the outer radius of hyperbolic disc2, the strain rates in this disc is the lowest as a result of the lowest effective stress (Figure 6).

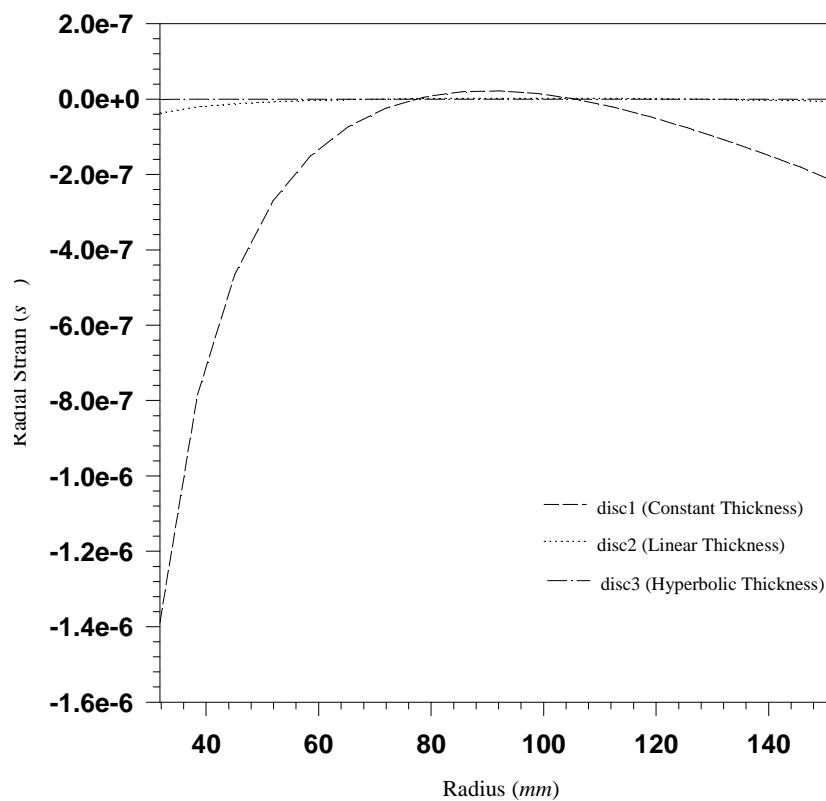


Figure 8. Effect of thickness profile on radial strain rate.

## CONCLUSIONS

The present study reveals that the creep stresses and strain rates in the FGM disc are significantly affected by varying the disc profile. The radial, tangential and effective stresses

in the FGM disc having hyperbolic thickness are significantly lower than those observed in FGM discs having uniform and linearly varying thickness. When a constant thickness FGM disc is replaced by similar FGM discs having linear and hyperbolic thickness profiles, the tangential strain rate reduces respectively by about two and three orders of magnitude. Similar effects are noticed for radial strain rate in the FGM disc. The FGM discs having linear and hyperbolic thickness profiles exhibit relatively uniform distribution of radial strain rate and hence possess lesser chances of distortion.

## References:

- [1] SINGH, S.B. and RAY, S., Modeling the anisotropy and creep in orthotropic aluminum-silicon carbide composite rotating disc, *Mechanics of Materials* **34** (2002) 363-372.
- [2] GUPTA, V.K., SINGH, S.B., CHANDRAWAT, H.N., and RAY, S., Modeling of creep behavior of a rotating disc in the presence of both composition and thermal gradients, *Journal of Engineering Materials and Technology* **127** (2005) 97-105.
- [3] HOJJATI, M.H. and HASSANI, A., Theoretical and numerical analysis of rotating discs of non-uniform thickness and density, *International Journal of Pressure Vessels and Piping* **5** (2008) 694-700.
- [4] FARSHI, B. and BIDABADI, J., Optimum design of inhomogeneous rotating discs under secondary creep, *International Journal of Pressure Vessels and Piping* **85** (2008) 507-515.
- [5] LASKAJ, M., MURPHY, B. and HOUNGAN, K., *Improving the efficiency of cooling the front disc brake on a V8 racing car*, Project report, Monash University, Melbourne (1999).
- [6] FARSHI, B., JAHED, H. and MEHRABIAN, A., Optimum design of inhomogeneous non-uniform rotating discs, *Computers and Structures* **82** (2004) 773-779.
- [7] GUPTA, V.K., KWATRA, N. and RAY, S., Artificial neural network modeling of creep behavior in a rotating composite disc, *Engineering Computations: International Journal for Computer-Aided Engineering and Software* **24** (2) (2007) 151-164.
- [8] SHARMA, S., SAHAI, I. and KUMAR, R., Creep transition of a thin rotating annular disk of exponentially variable thickness with inclusion and edge load, *Procedia Engineering* **55** (2013) 348-354.
- [9] NIEH, T.G., XIA, K. and LANGDON, T.G., Mechanical properties of discontinuous SiC reinforced aluminium composites at elevated temperatures, *Journal of Engineering Materials and Technology* **110** (1998) 77-82.
- [10] SURESH, S. and MORTENSEN, A., *Fundamentals of Functionally Graded Materials*, IOM Communications Limited, London, U.K. (1998).
- [11] REDDY, J.N., Analysis of functionally graded plates, *International Journal of Numerical Method Engineering* **47** (2000) 663-684.
- [12] DEEPAK, D., GUPTA, V.K. and DHAM, A.K., Creep modeling in functionally graded rotating disc of variable thickness, *Journal of Mechanical Science and Technology* **24** (2010) 2221-2232.
- [13] SINGH, S.B. and RAY, S., Steady state creep behavior in an isotropic functionally graded material rotating disc of Al-SiC composite, *Metallurgical and Materials Transactions* **A32** (2001) 1679-1685.

- [14] GUPTA, V.K., SINGH, S.B., CHANDRAWAT, H.N. and RAY, S., Creep behavior of a rotating functionally graded composite disc operating under thermal gradients, *Metallurgical and Materials Transactions A* **35** (2004) 1381-1391.
- [15] YOU, L.H., YOU, X., ZHANG, J.J. and LI, J., On rotating circular disks with varying material properties, *Zeitschrift für angewandte Mathematik und Physik* **58** (2007) 1068-1084.
- [16] CHEN, J., DING, H. and CHEN, W., Three-dimensional analytical solution for a rotating disc of functionally graded materials with transverse isotropy, *Archive of Applied Mechanics* **77** (2007) 241-251.
- [17] BAYAT, M.N., SALEEM, M., SAHARI, B.B., HAMOUDA, A.M.S. and MAHDI, E., Thermo elastic analysis of a functionally graded rotating disk with small and large deflections, *Thin-Walled Structures* **45** (2007) 677-691.
- [18] BAYAT, M., SALEEM, M., SAHARI, B.B., HAMOUDA, A.M.S. and MAHDI, E., Analysis of functionally graded rotating discs with variable thickness, *Mechanics Research Communications* **35** (2008) 283-309.
- [19] KORDKHEILI, S.A.H. and NAGHDABADI, R., Thermo elastic analysis of a functionally graded rotating disk, *Composite Structures* **79** (2007) 508-516.
- [20] ORCAN, Y. and ERASLAN, A.N., Elastic-plastic stresses in linearly hardening rotating solid disks of variable thickness, *Mechanics Research Communications* **29** (2002) 269-281.
- [21] JAHED, H., FARSHI, B. and BIDABADI, J., Minimum weight design of inhomogeneous rotating discs, *International Journal of Pressure Vessels and Piping* **82** (2005) 35-41.
- [22] GUPTA, S.K., SHARMA, S., and PATHAK, S., Creep transition in a thin rotating disc having variable thickness and variable density, *Indian Journal of Pure Applied Mathematics* **3** (2000) 1235-1248.
- [23] ALI, A., BAYAT, M., SAHARI, B.B., SALEEM, M. and ZAROOG, O.S., The effect of ceramic in combinations of two sigmoid functionally graded rotating disks with variable thickness, *Scientific Research and Essays* **7** (2012) 2174-2188.
- [24] HASSANI, A., HOJJATI, M.H., FARRAHI, G.H., and ALASHTI, R.A., Semi-exact solution for thermo-mechanical analysis of functionally graded elastic-strain hardening rotating disks, *Communications in Nonlinear Science and Numerical Simulation* **17** (2012) 3747-3762.
- [25] THAKUR, P., SINGH, S.B. and KAUR, J., Elastic-plastic stresses in a thin rotating disk with shafthaving density variation parameter under steady-state temperature, *Kragujevac Journal of Science* **36** (2014) 5-17.
- [26] TJONG, S.C. and MA, Z.Y., Microstructural and mechanical characteristics in situ metal matrix composites, *Materials Science and Engineering* **29** (2000) 49-113.
- [27] MA, Z.Y. and TJONG, S.C., Creep deformation characteristics of discontinuously reinforced aluminium matrix composites, *Composites Science and Technology* **61** (2001) 771-786.
- [28] PANDEY, A.B., MISHRA, R.S. and MAHAJAN, Y.R., High-temperature creep of Al-TiB<sub>2</sub> particulate composites, *Materials Science and Engineering* **189A** (1994) 95-104.
- [29] TIMOSHENKO, S.P. and GOODIER, J.N., *Theory of Elasticity*, McGraw-Hill, Singapore (1970).

Table 1. Creep parameters used for Al-SiCp in the present study.

| $P$<br>( $\mu m$ ) | $T$<br>(K) | $V$<br>(vol. %) | $M$<br>( $s^{-1/5}/MPa$ ) | $\sigma_0$<br>(MPa) | Coefficient of<br>Correlation |
|--------------------|------------|-----------------|---------------------------|---------------------|-------------------------------|
| 1.7                | 623        | 10              | 4.35E-03                  | 19.83               | 0.945                         |
| 14.5               |            |                 | 8.72E-03                  | 16.50               | 0.999                         |
| 45.9               |            |                 | 9.39E-03                  | 16.29               | 0.998                         |
| 1.7                | 623        | 10              | 4.35E-03                  | 19.83               | 0.945                         |
|                    |            | 20              | 2.63E-03                  | 32.02               | 0.995                         |
|                    |            | 30              | 2.27E-03                  | 42.56               | 0.945                         |
| 1.7                | 623        | 20              | 2.63E-03                  | 32.02               | 0.995                         |
|                    | 673        |                 | 4.14E-03                  | 29.79               | 0.974                         |
|                    | 723        |                 | 5.92E-03                  | 29.18               | 0.916                         |